ELSEVIER

Journal of Photochemistry and Photobiology A: Chemistry 137 (2000) 177–184

Journal of Photochemistry and Photobiology A:Chemistry

www.elsevier.nl/locate/jphotochem

Hydroxyl radical initiated photodegradation of 4-chloro-3,5-dinitrobenzoic acid in aqueous solution

Jorge L. Lopez [a], Fernando S. García Einschlag [a], Mónica C. González [a], Alberto L. Capparelli [a], Esther Oliveros [b], Tarek M. Hashem [b], André M. Braun*

[a] *Instituto de Investigaciones Fisicoquímicas Teóricas y Aplicadas, Facultad de Ciencias Exactas, Universidad Nacional de La Plata, Casilla de Correo 16, Sucursal 4, (1900) La Plata, Argentina*

[b] *Lehrstuhl für Umweltmesstechnik, Engler-Bunte-Institut, Universität Karlsruhe, D-76128 Karlsruhe, Germany*

Received 21 August 2000; accepted 23 August 2000

Abstract

The photodegradation of 4-chloro-3,5-dinitrobenzoic acid (CDNBA) in aqueous solution was investigated using advanced oxidation processes (AOP) involving hydroxyl radical production: (i) UV-C photolysis of H_2O_2 using low or medium pressure Hg arcs (UV/H_2O_2 process) and (ii) vacuum ultraviolet (VUV) photolysis of water at 185 nm (low pressure Hg arc with Suprasil envelope) and at 172 nm (Xe-excimer lamp). These processes were shown to be efficient methods for CDNBA mineralization, in contrast to CDNBA photolysis. For the UV/H_2O_2 process, the optimal concentration of H_2O_2 leading to the fastest degradation rate could be evaluated as a function of the initial CDNBA concentration using a simplified equation based on the main reactions involved in the first stages of the degradation process. Chloride ions were produced at the same rate as CDNBA was depleted, independently of the method used for the production of hydroxyl radicals. In contrast, the production of nitrate and nitrite ions was strongly process dependent, the differences being related to the formation of primary reducing intermediates by VUV photolysis of water.

Keywords: Advanced oxidation processes (AOP); Chloronitro aromatic compounds; Hydroxyl radical; UV/H_2O_2 process; VUV photolysis; Excimer lamps

1. Introduction

Various advanced oxidation processes (AOP) are nowadays available and applicable at laboratory, pilot or even technical levels for achieving oxidative degradation of organic pollutants in aqueous media. Most of these processes are based on the production of hydroxyl radicals as primary oxidizing species. The reaction of hydroxyl radicals with organic compounds (by addition to double bonds and/or by hydrogen abstraction) generates C-centered organic radicals that are subsequently trapped by dissolved molecular oxygen to yield peroxides and peroxyl radicals. These intermediates initiate thermal chain autooxidation reactions and the overall process may eventually lead to complete mineralization (to CO_2, H_2O and mineral acids). Among AOP processes based on the production of hydroxyl radicals, combination of UV irradiation and oxidants (hydrogen peroxide, ozone), TiO_2 photocatalysis or vacuum ultraviolet (VUV) photolysis of water have proven useful for destroying a large variety of organic contaminants (see e.g. [1–10]). It should be noted that photodegradation of a primary pollutant by photochemical and thermal pathways most often results in the formation of a series of products which may themselves be more or less toxic, and therefore further degradation may be required.

Nitrogen containing organic intermediates or by-products are in many cases toxic and hazardous for the environment, and various techniques for their photochemical degradation have been investigated [1,9–11]. The aim of this work was to study the efficiency of the UV/H_2O_2 and the VUV processes when applied to the degradation of nitroaromatics in aqueous solution. In particular, we have been interested in nitrobenzoic acids formed as intermediates in the photodegradation of nitrotoluenes [12]. The substrate investigated was 4-chloro-3,5-dinitrobenzoic acid (CDNBA) which is known to be irritant in contact with the skin, eyes and to inhibit the growth of micro-organisms at concentrations higher than 30 mg l^{-1}.

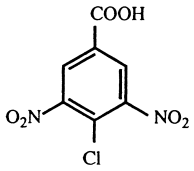

(CDNBA)

* Corresponding author. Tel.: +49-721-6082557; fax: +49-721-6086240.
E-mail address: Andre.Braun@ciw.uni-karlsruhe.de (A.M. Braun).

1010-6030/00/$ – see front matter
PII: S1010-6030(00)00357-9

2. Experimental section

2.1. Chemicals

CDNBA (Aldrich) is a yellow solid at room temperature. However, it slowly decomposes during storage as shown by the changes in color (yellow to brownish) and melting point. Therefore, as recommended in the literature [13], CDNBA was purified by several recrystallizations from mixtures of ethyl alcohol and water, until the melting temperature was in the range from 159 to 162°C. CDNBA is only slightly soluble in water, and its concentration was limited to 5×10^{-4} mol l^{-1}.

Hydrogen peroxide (30% H_2O_2 w/w in aqueous solution) was purchased from Merck (30% perhydrol). The concentrations of H_2O_2 (5.5×10^{-3} to 0.6 mol l^{-1}) were checked by titration with $KMnO_4$.

2.2. Photochemical reactors

The experiments were performed in two different annular photochemical reactors. One of the reactors (DEMA, Mangels, Bornheim–Roisdorf, Germany) had a capacity of 1 l and was equipped with a medium pressure mercury lamp (Philips HPK 125 W) positioned in the axis of the reactor. The second reactor had a capacity of 350 ml (thickness 8 mm) and could be operated with different types of light sources of comparable size mounted in the axis of a Suprasil quartz tube; (i) a conventional low pressure mercury arc emitting at 254 nm (MNNI 35/20, Heraeus Noblelight, "ozone protected", electrical power of 35 W), (ii) a low pressure mercury arc with Suprasil envelope (NIQ 40/18, Heraeus Noblelight, electrical power of 50 W) allowing irradiation at 185 as well as 254 nm, and (iii) a xenon excimer lamp with an emission maximum at 172 nm with a half-width of less than 14 nm [14–19] and operated with an electrical power input of 130 W. The incident rates of photons emitted by the low pressure mercury arc (with Suprasil envelope) at 185 nm and by the xenon excimer lamp at 172 nm were $1.3(\pm0.1) \times 10^{-5}$ einstein l^{-1} s^{-1} (radiant power of 3 W) and $1.9(\pm0.2) \times 10^{-5}$ einstein l^{-1} s^{-1} (radiant power of 4.5 W), respectively, as determined by VUV actinometric procedures [17–19]) in the 350 ml reactor. A value of $2.1(\pm0.2) \times 10^{-5}$ einstein l^{-1} s^{-1} was obtained for the incident photonic rate of the low pressure mercury arc at 254 nm, using uranyl oxalate actinometry [20]. The reactors were made out of Pyrex and equipped with a stirring system, ports for sample withdrawing and purging gases. Solutions were continuously purged with synthetic air and the temperature maintained at 25°C (±1°C). Hydrogen peroxide was introduced at once in the reactor just before starting the irradiation.

2.3. Analyses

Absorption spectra were registered on a Cary 3 spectrophotometer. The molar absorption coefficient of CDNBA at 254 nm was determined to be 7670 ± 280 l mol^{-1} cm^{-1}. For concentrations of H_2O_2 lower than 0.08 mol l^{-1}, initial rates of CDNBA disappearance could be determined by following the decrease of CDNBA absorbance above 300 nm without interference due to H_2O_2 absorption. Measurements of pH of the irradiated solutions were performed using a Radiometer pH meter.

HPLC analyses were carried out using the following equipment and experimental conditions: HP1050 Ti-series equipped with a LiChrospher 100 RP-18 column (length 125 mm, diameter 4 mm, film thickness 5 mm) for the CDNBA analysis, the eluent was a mixture of methanol and water 15/85 at a flow rate of 1–2 ml/min.

Ion chromatography (IC) measurements of chloride, nitrite, and nitrate were performed on the same instrument using a IONPAC AS12A DIONEX column (length 200 mm, diameter 4 mm), an aqueous solution of sodium carbonate (2.7×10^{-3} mol l^{-1}) and sodium bicarbonate (3×10^{-4} mol l^{-1}) was employed as an eluent at a flow rate of 1.5 ml/min. Within experimental error, the same results were obtained for nitrite evolution by calorimetric measurements using the Illosva or Griess reagents [21,22] and by IC.

Dissolved organic carbon (DOC) (Dohrmann DC-190, Rosemount Analytic, oven temperature of 680°C and Beckman Tocamaster 915-B, oven temperature 950°C) measurements were also carried out on the various samples. The experimental error on DOC values was ±8%.

3. Results and discussion

3.1. Photolysis of CDNBA

The absorption spectrum of CDNBA in aqueous solution is shown in Fig. 1. Under the experimental conditions used in this work, the pH ranged from 3.9 to 5.0. CDNBA is not stable under alkaline conditions, as shown by the changes in the absorption spectrum (Fig. 1). At pH higher than 7, solutions develop an intense yellow coloration, most probably due to the formation of phenolate derivatives by

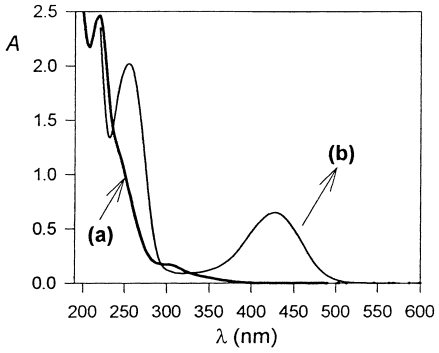

Fig. 1. Absorption spectra of CDNBA in aqueous solution: (a) pH 3.92, and (b) after alkalinization at pH 12.8 ([CDNBA]$_0 = 1.1 \times 10^{-4}$ mol l^{-1}, ionic strength ($NaClO_4$) 2.5 mol l^{-1}).

nucleophilic substitution of the chloride by the hydroxide ion [23,24] (the absorption band between 350 and 500 nm is typical of phenolic derivatives).

Irradiation of aqueous solutions of CDNBA ($[CDNBA]_0 = 5.0 \times 10^{-4}$ mol l^{-1}) using conventional low or medium pressure mercury arcs (Section 2.2) yielded inefficient substrate photolysis (Fig. 2).

The quantum yield of CDNBA disappearance under monochromatic irradiation at 254 nm (Eq. (1)) was evaluated by combining uranyl oxalate actinometry for the determination of the incident photonic rate [20] and measurements of the CDNBA concentration by HPLC (Section 2.3).

$$\Phi_{-\mathrm{CDNBA}} = \frac{-\mathrm{d[CDNBA]/d}t}{P_\mathrm{a}^{\mathrm{CDNBA}}} = \frac{-\mathrm{d[CDNBA]/d}t}{P_0(1-10^{-A_{\mathrm{CDNBA}}})} \quad (1)$$

where $-$d[CDNBA]/dt is the rate of CDNBA disappearance (mol l^{-1} s^{-1}), $P_\mathrm{a}^{\mathrm{CDNBA}}$ is the rate of photons absorbed by CDNBA (einstein l^{-1} s^{-1}); P_0 is the incident photonic rate (2.1×10^{-5} einstein l^{-1} s^{-1}, 350 ml annular reactor, Section 2.2); $A_{\mathrm{CDNBA}} = \varepsilon_{\mathrm{CDNBA}}\, d[\mathrm{CDNBA}]$ is the absorbance of CDNBA at the wavelength of irradiation, with $\varepsilon_{\mathrm{CDNBA}}$, molar absorption coefficient and d, optical path length.

Under our experimental conditions, CDNBA disappearance was slow and followed apparent pseudo-zero-order kinetics during the whole irradiation period. The corresponding pseudo-zero-order rate constant was calculated to be $3.6(\pm 0.3) \times 10^{-9}$ l mol^{-1} s^{-1} under irradiation at 254 nm (Fig. 2). With an initial concentration of CDNBA of 5×10^{-4} mol l^{-1}, the absorbance of CDNBA was larger than 2 (total absorption) during the whole irradiation time, and the rate of photons absorbed by CDNBA was equal to the incident photonic rate ($P_\mathrm{a}^{\mathrm{CDNBA}} = P_0$, Eq. (1)). Under these conditions, a value of $1.7(\pm 0.2) \times 10^{-4}$ was obtained for the apparent quantum yield of CDNBA disappearance ($\Phi_{-\mathrm{CDNBA}}^{\mathrm{ap}}$). Within experimental error, no significant depletion of the dissolved organic carbon (DOC) could be observed after more than 4 h of irradiation.

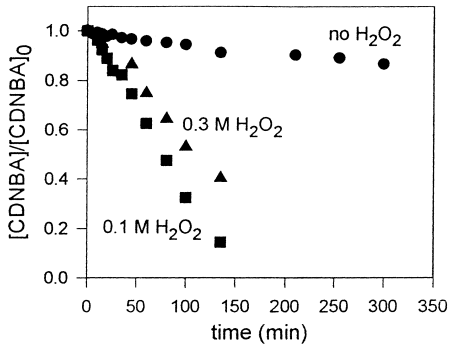

Fig. 2. CDNBA concentration profiles as a function of irradiation time in the absence of H_2O_2 (filled circles) and in the presence of H_2O_2, 0.1 mol l^{-1} (squares) and 0.3 mol l^{-1} (triangles); ($[CDNBA]_0 = 5.0 \times 10^{-4}$ mol l^{-1}, i.e. 42 mg C l^{-1}, 350 ml annular photoreactor, irradiation at 254 nm, see Section 2.2).

3.2. UV/H_2O_2 process

3.2.1. CDNBA degradation by the UV/H_2O_2 process

Irradiation of aqueous solutions of CDNBA in the presence of H_2O_2 led to a more efficient CDNBA degradation than in the absence of H_2O_2 (Fig. 2), and the DOC was depleted, albeit at a lower rate than CDNBA disappearance (see Fig. 3(b) as a typical example).

Photolysis of H_2O_2 produces hydroxyl radicals (reaction 2). The quantum yield of H_2O_2 photodissociation in aqueous solution has been reported to be about 0.5 (or lower) due to the recombination reactions resulting from the cage effect [25].

$$H_2O_2 \xrightarrow{h\nu} 2HO^\bullet \quad (2)$$

Although increasing steadily at shorter wavelengths, the molar absorption coefficient of hydrogen peroxide ($\varepsilon_{\mathrm{HP}}$) at 254 nm is only 18.7 L mol^{-1} cm^{-1} [25]. Therefore, absorption of incident radiation by CDNBA competes with absorption by H_2O_2. Under conditions where CDNBA photolysis may be neglected, the quantum yield of CDNBA disappearance in the presence of H_2O_2 ($\Phi_{-\mathrm{CDNBA}}^{\mathrm{HP}}$) may be calculated as

$$\Phi_{-\mathrm{CDNBA}}^{\mathrm{HP}} = \frac{-\mathrm{d[CDNBA]/d}t}{P_\mathrm{a}^{\mathrm{HP}}} \quad (3)$$

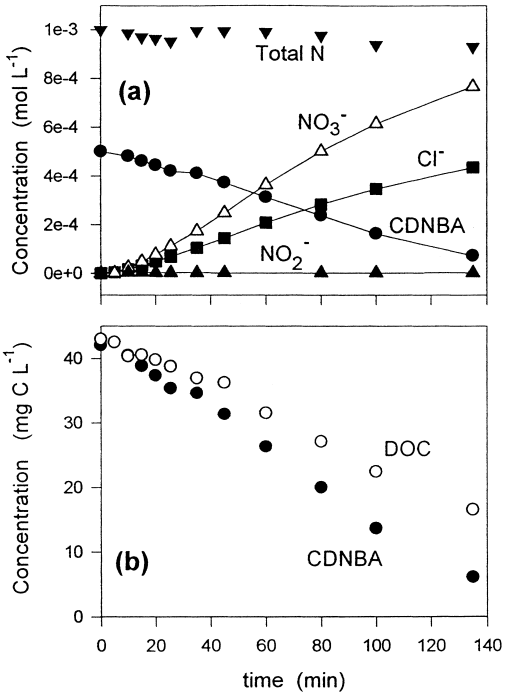

Fig. 3. Degradation of CDNBA by the UV/H_2O_2 process: (a) concentration profiles in mol l^{-1} of CDNBA (filled circles), chloride (squares), nitrate (open triangles), nitrite (filled triangles) and total nitrogen (mol l^{-1} of N) as a function of irradiation time; (b) concentration profiles in mg C l^{-1} of CDNBA and DOC (open circles); ($[CDNBA]_0 = 5.0 \times 10^{-4}$ mol l^{-1}, i.e. 42 mg C l^{-1}, $[H_2O_2]_0 = 0.1$ mol l^{-1}, 350 ml annular photoreactor, irradiation at 254 nm, see Section 2.2).

where $P_a^{HP} = P_0(1 - 10^{-A_t})(A_{HP}/A_t)$ is the rate of photons absorbed by H_2O_2 (einstein l^{-1} s^{-1}); with A_{HP}/A_t, fraction of incident radiation absorbed by H_2O_2; and $A_t = A_{HP} + A_{CDNBA} = d(\varepsilon_{HP}[HP] + \varepsilon_{CDNBA}[CDNBA])$, total absorbance.

Using initial concentrations of 5×10^{-4} mol l^{-1} for CDNBA and 0.1 mol l^{-1} for H_2O_2, 33% of the incident radiation (254 nm) is absorbed by H_2O_2 at the beginning of the irradiation time. As the reaction proceeds, both total absorbance and fraction of incident radiation absorbed by H_2O_2 are modified. Nevertheless, the evolution of the CDNBA concentration could be well approximated by pseudo-zero-order kinetics. Under the initial conditions mentioned above, the pseudo-zero-order rate constant of CDNBA disappearance was determined to be $5.5(\pm0.4) \times 10^{-8}$ mol l^{-1} s^{-1} (Fig. 2). Taking into account Φ_{-CDNBA}^{HP} in the absence of H_2O_2 (Section 3.1) and the initial rate of photons absorbed by CDNBA in the presence of 0.1 mol l^{-1} of H_2O_2 (67% of P_0), the contribution of CDNBA photolysis to CDNBA disappearance was within the limits of experimental error. The value obtained for Φ_{-CDNBA}^{ap} at the beginning of the irradiation time was then $7.9(\pm0.8) \times 10^{-3}$, i.e. more than 45 times larger than in the absence of H_2O_2. When the concentration of H_2O_2 was increased to 0.3 mol l^{-1}, the fraction of incident radiation absorbed by H_2O_2 at the beginning of the irradiation time increased to 60%. However, the rate of CDNBA disappearance and the corresponding apparent quantum yield decreased to $3.9(\pm0.3) \times 10^{-8}$ mol l^{-1} s^{-1} and $3.1(\pm0.3) \times 10^{-3}$, respectively (Fig. 2). This effect is discussed in the following section.

3.2.2. Effect of the concentration of H_2O_2

The efficiency of CDNBA degradation and DOC depletion were strongly dependent on the H_2O_2 concentration (Figs. 2 and 4), DOC depletion being slower than that of CDNBA disappearance (Fig. 3(b)).

The degradation rate for both CDNBA and DOC increased with increasing initial H_2O_2 concentration up to a maximum

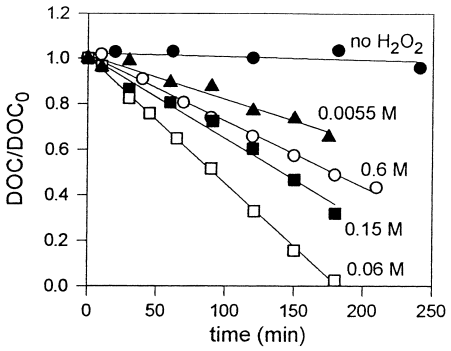

Fig. 4. Degradation of CDNBA by the UV/H_2O_2 process: evolution of the relative DOC as a function of irradiation time at different initial H_2O_2 concentrations; ([CDNBA]$_0$ = 5.0×10^{-4} mol l^{-1}, i.e. 42 mg C l^{-1}, 1 l annular photoreactor, medium pressure mercury arc, see Section 2.2).

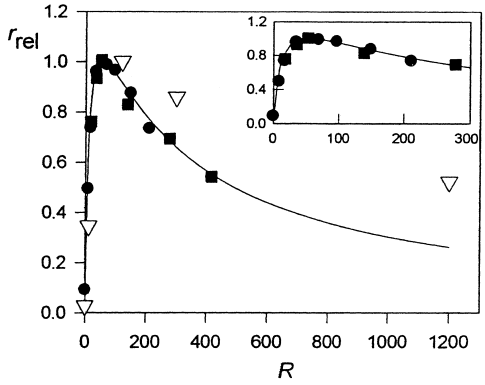

Fig. 5. Degradation of CDNBA by the UV/H_2O_2 process: relative rates of CDNBA and DOC disappearance as a function of R ([HP]$_0$/[CDNBA]$_0$): [CDNBA]$_0$ = 3.3×10^{-4} mol l^{-1} (squares), 1.6×10^{-4} mol l^{-1} (dots), best fit to Eq. (10) is also shown; DOC (inverted triangles, [CDNBA]$_0$ = 5.0×10^{-4} mol l^{-1}, see also Fig. 4); (1 l annular photoreactor, medium pressure mercury arc, see Section 2.2).

value, then decreased when larger amounts of H_2O_2 were added (Figs. 2, 4 and 5). The existence of such a maximum results from the competing reactions of hydroxyl radicals with the organic substrate (reaction 4) and H_2O_2 (reaction 5).

$$\text{CDNBA} + \text{HO}^\bullet \xrightarrow{k_{CDNBA}} \text{intermediates} \quad (4)$$

$$\text{H}_2\text{O}_2 + \text{HO}^\bullet \xrightarrow{k_{HP}} \text{HO}_2^\bullet + \text{H}_2\text{O} \quad (5)$$

As the initial H_2O_2 concentration is increased, the fraction of incident radiation absorbed by H_2O_2 increases, leading to an increased production of $HO^\bullet$, but at the same time reaction 5 is getting more competitive with respect to reaction 4. It should be noted that hydroperoxyl radicals ($HO_2^\bullet$) produced by reaction 5 are much less reactive than $HO^\bullet$ [26]. The optimal concentration of H_2O_2 represents the best compromise between the fraction of incident radiation absorbed by H_2O_2 and the trapping of $HO^\bullet$ by the additive itself. A value of 3.3×10^7 l mol^{-1} s^{-1} was published for the bimolecular rate constant of the reaction between H_2O_2 and $HO^\bullet$ [27]. Bimolecular rate constants published for the reactions between $HO^\bullet$ and chlorobenzene, nitrobenzene, 1-chloro-4-nitrobenzene, 4-chlorobenzoate, benzoic acid are 5.6×10^9 l mol^{-1} s^{-1} (293 K) [28], 3.9×10^9 l mol^{-1} s^{-1} [25], 1.3×10^9 l mol^{-1} s^{-1} [29], 5.0×10^9 l mol^{-1} s^{-1} [30], and 4.3×10^9 l mol^{-1} s^{-1}, respectively [25].

Assuming a simplified reaction scheme including reactions 2, 4 and 5, the CDNBA degradation rate under photostationary conditions (pseudo-steady-state assumption) is given by

$$r = \frac{-\text{d[CDNBA]}}{\text{d}t} = k_{CDNBA}[\text{CDNBA}][\text{HO}^\bullet]_{st} \quad (6)$$

where the stationary concentration of hydroxyl radicals ($[HO^\bullet]_{st}$) can be expressed as

$$[\text{HO}^\bullet]_{st} = \frac{P_a^{HP}\Phi_{HO^\bullet}}{(k_{CDNBA}[\text{CDNBA}] + k_{HP}[\text{HP}])} \quad (7)$$

where $\Phi_{HO^\bullet}$ is the quantum yield of $HO^\bullet$ production by H_2O_2 photolysis.

Under conditions of total absorption of the incident radiation, a simplified expression for the rate (r) may be written (Eq. (8)).

$$r = \frac{\Phi_{HO^\bullet} P_0 \varepsilon_{HP}[HP] k_{CDNBA}[CDNBA]}{(\varepsilon_{HP}[HP] + \varepsilon_{CDNBA}[CDNBA]) \times (k_{CDNBA}[CDNBA] + k_{HP}[HP])} \quad (8)$$

For a given substrate concentration ($[CDNBA]_0$), the optimal concentration of H_2O_2 (denoted as $[HP]_{op}$) leading to a maximum initial rate of substrate degradation may be calculated by derivation (Eq. (9a) and (9b)). A similar approach was proposed recently by D.F. Ollis for the optimal dosing of H_2O_2 [31].

$$[HP]_{op} = [CDNBA]_0 \left\{ \frac{(k_{CDNBA}\varepsilon_{CDNBA})}{(k_{HP}\varepsilon_{HP})} \right\}^{1/2} \quad (9a)$$

or

$$R_{op}^2 = \frac{k_{CDNBA}\varepsilon_{CDNBA}}{k_{HP}\varepsilon_{HP}} \quad (9b)$$

Under conditions where the simplified scheme may be applied, the optimal ratio of the initial concentrations of H_2O_2 and CDNBA (R_{op}) should not depend on $[CDNBA]_0$. We have measured the initial rates of CDNBA disappearance as a function of R ($[HP]_0/[CDNBA]_0$) for two different values of $[CDNBA]_0$ (3.3×10^{-4} mol l^{-1} and 1.6×10^{-4} mol l^{-1}). The results are shown in Fig. 5. For both series of experiments, the value of R_{op} is in the range of 50–70. Therefore, an estimated value of k_{CDNBA} between 2.0×10^8 and 3.9×10^8 l mol^{-1} s^{-1} may be calculated using Eq. (9a) or (9b).

Relative initial rates of CDNBA disappearance in a given series of experiments (i.e. same irradiation source and reactor geometry) may be evaluated using Eq. (10), directly derived from Eq. (8).

$$r_{rel} = \frac{r}{r_M} = \frac{D_M R}{R_M D} = \frac{aR}{(1+bR)(1+cR)} \quad (10)$$

where $D = (1 + bR)\ (1 + cR)$ and subscript M refers to the experiment taken as a reference (in this case, $r_M = r_{max}$), $b = k_{HP}/k_{CDNBA}$, $c = \varepsilon_{HP}/\varepsilon_{CDNBA}$ and $a = D_M/R_M$.

Within experimental error, values of r_{rel} for CDNBA disappearance as a function of R yield the same curve independently of $[CDNBA]_0$. The best fit of the ensemble of experimental points to Eq. (10) (Fig. 5) is obtained for $k_{CDNBA} = 3.5 \times 10^8$ l mol^{-1} s^{-1} ($R_{op} = 66$). This value is significantly smaller than that reported for the rate constant of reaction between $HO^\bullet$ and 1-chloro-4-nitrobenzene (1.3×10^9 l mol^{-1} s^{-1} [29]). This result is in agreement with Ho's observation that 2,4-dinitrobenzoic acid has a lower reactivity towards $HO^\bullet$ than 2,4-dinitrotoluene [11]. It should be noted that the variation of r_{rel} is relatively flat around R_{op} (Fig. 5, inset): for values of R between 35 and 100, the variation of r_{rel} does not exceed 5%. Moreover, the variation of r_{rel} is asymmetrical, i.e. decreasing R below R_{op} leads to a sharper decrease of r_{rel} than increasing its value above R_{op} by a similar amount (Fig. 5, inset).

The experimental values of r_{rel} obtained for the DOC depletion follow a similar trend (Fig. 5). However, the optimal value of R_{op} for DOC depletion seems to be higher than that observed for CDNBA, probably due to the fact that mineralization involves oxidation of the various intermediate products formed upon CDNBA degradation.

Under the experimental conditions reported in Section 3.2.1, calculated values of the efficiencies of the reaction of $HO^\bullet$ with CDNBA (ϕ_{CDNBA}) at the beginning of the irradiation time,

$$\phi_{CDNBA} = \frac{k_{CDNBA}[CDNBA]_0}{k_{CDNBA}[CDNBA]_0 + k_{HP}[HP]_0}$$

are equal to 0.050 and 0.017 for $[HP]_0$ of 0.1 mol l^{-1} and 0.3 mol l^{-1}, respectively. Note that the ratio of these efficiencies (2.9) is close to the ratio of the corresponding apparent quantum yields of CDNBA disappearance (2.5) (Section 3.2.1), as expected if the simplified scheme may be considered as an acceptable approximation.

We are currently testing Eqs. (9a), (9b) and (10) for a more general application in the H_2O_2/UV process, (i) for an evaluation of rate constants associated with the interaction between $HO^\bullet$ radicals and organic substrates by determining experimentally the optimal H_2O_2 concentrations, or (ii) for the calculation of the optimal H_2O_2 concentration to be applied when the corresponding rate constant is known.

3.2.3. Products of CDNBA degradation during the UV/H_2O_2 process

CDNBA degradation and DOC depletion during irradiation in the presence of H_2O_2 led to an increase in the conductivity of the solution and a decrease of pH, as mineral acids (HCl, HNO_3) were formed. As expected, pH diminution was the fastest at the optimum H_2O_2 concentration (data not shown). A typical example of the evolution of chloride, nitrite and nitrate during irradiation is given in Fig. 3(a). IC experiments showed that chloride ions were released at the same rate as CDNBA disappeared. This result may be explained by a mechanism involving electrophilic attack of $HO^\bullet$ on the carbon atom substituted by Cl followed by HCl elimination, as already proposed for the oxidation of 4-chlorophenol by hydroxyl radicals [8].

A similar mechanism would lead to the elimination of HNO_2, following electrophilic addition of $HO^\bullet$ to the carbon atoms substituted by the nitro group. It has been already shown that the addition of a hydroxyl radical may take place at various sites of an aromatic nucleus (see e.g. [11,32]. The C-centered radicals formed may be trapped by O_2, and react further with $HO^\bullet$ or $HO_2^\bullet$, leading to the formation of various unstable highly oxidized intermediates which undergo ring opening at an early reaction stage. This interpretation is in agreement with the fact that no aromatic intermediates

could be detected by HPLC. Nitrite concentration was at the limits of detection. In fact, nitrite is efficiently oxidized to nitrate by H_2O_2 and hydroxyl radicals [33]. Nitrate formation was slightly delayed in comparison to that of chloride. However, within experimental error, the amount of nitrate was never more than 10% below the stoichiometric molar ratio of 2/1 that would be expected if all the CDNBA nitrogen content was mineralized to nitrate (two nitrate ions formed per molecule of CDNBA mineralized). The nitrogen balance is shown in Fig. 3 in the case of an initial H_2O_2 concentration of 0.1 mol l^{-1}. The formation of chloride and nitrate in molar stoichiometric ratios with respect to CDNBA disappearance was also observed using 0.3 mol l^{-1} of H_2O_2 (data not shown).

3.3. VUV process

3.3.1. CDNBA degradation by VUV photolysis of water

Water absorbs strongly at wavelengths lower than 190 nm, the absorption cross section increasing as the wavelength decreases between 190 and 160 nm [19]. We have used two types of VUV irradiation sources, a low pressure mercury arc with Suprasil envelope allowing irradiation at 185 nm and a xenon-excimer lamp emitting at 172 nm (Section 2.2). It should be noted that, due to the high absorption cross section of water, the whole incident radiation is absorbed within a very narrow layer around the lamp shaft (approx. 100 and 300 μm at 172 and 185 nm, respectively) [18,34,35].

Under VUV irradiation, water molecules are dissociated in H atoms, hydroxyl radicals and hydrated electrons (e^-_{aq}), as described by reactions 11 and 12.

$$H_2O \xrightarrow{h\nu} H^\bullet + HO^\bullet \quad (11)$$

$$H_2O \xrightarrow{h\nu} H^+ + HO^\bullet + e^-_{aq} \quad (12)$$

The quantum yield for the production of solvated electrons is low (0.05), being almost independent of the wavelength in the range 160–190 nm. In contrast, the quantum yield of $HO^\bullet$ production ($\Phi_{HO^\bullet}$) is wavelength dependent [18,19,33] and decreases with increasing irradiation wavelength. Values of 0.42(±0.03) and 0.33(±0.03) at 172 and 185 nm, respectively, have been reported [19]. In aerated solutions, H atoms and hydrated electrons are efficiently trapped by oxygen, yielding hydroperoxyl radicals ($HO_2^\bullet$) and its conjugated base, the superoxide anion.

Irradiation of an aerated aqueous solution of CDNBA using the Xe-excimer lamp led to CDNBA degradation and DOC depletion at faster apparent rates than the UV/H_2O_2 process at the same CDNBA concentration (Fig. 6). The initial rate of CDNBA disappearance was $2.0(\pm0.2) \times 10^{-7}$ mol l^{-1} s^{-1}, with an incident photon rate at 172 nm of $1.9(\pm0.2) \times 10^{-5}$ einstein l^{-1} s^{-1} (Section 2.2). Therefore, the initial apparent quantum yield of CDNBA disappearance was $1.1(\pm0.1) \times 10^{-2}$.

The disappearance of CDNBA and the DOC depletion were slightly slower under VUV irradiation at 185 nm than at 172 nm (Figs. 6 and 7). The apparent quantum yield of CDNBA disappearance at 185 nm was $0.90(\pm0.09) \times 10^{-2}$. This slightly lower value of Φ_{-CDNBA} may result from the lower $\Phi_{HO^\bullet}$ at 185 nm (0.33) than at 172 nm (0.42).

The efficiency of trapping of $HO^\bullet$ radicals by CDNBA may be deduced from the values of Φ_{-CDNBA} and $\Phi_{HO^\bullet}$. A low value is obtained at both wavelengths (approx. 0.025). This result is in agreement with earlier observations. In the case of methanol (for which a rate constant of reaction with $HO^\bullet$ radicals of 10^9 l mol^{-1} s^{-1} has been published), a concentration of 0.2 mol l^{-1} was needed to trap all the $HO^\bullet$ radicals produced [19]. In fact the limited penetration of the VUV radiation in water (vide supra) leads to the formation of relative high concentrations of short lived $HO^\bullet$ radicals (greater than 10^{-4} mol l^{-1}) in a narrow layer around the lamp shaft and diffusion is not fast enough to avoid depletion of the substrate in this layer. Depletion of molecular oxygen in a thin layer around a 172 nm excimer lamp has been demonstrated experimentally [35].

3.3.2. Products of CDNBA degradation during VUV irradiation

During VUV photolysis of water, both at 172 and 185 nm, chloride ions were produced in stoechiometric amounts relative to the CDNBA consumed (Figs. 6 and 7), as observed

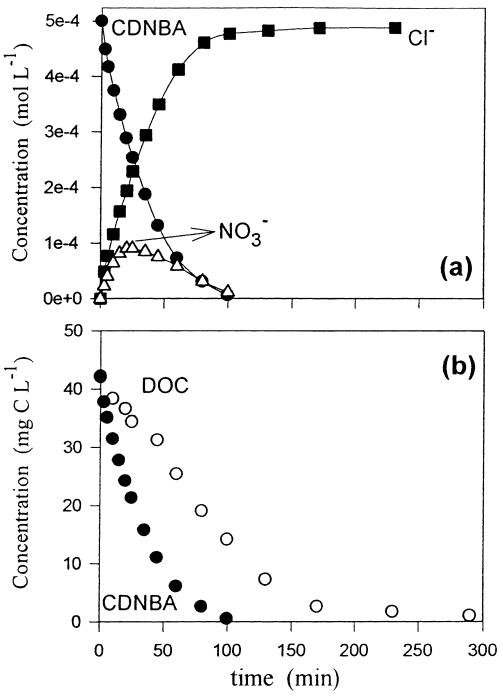

Fig. 6. Degradation of CDNBA by VUV photolysis of water at 172 nm: (a) concentration profiles in mol l^{-1} of CDNBA (filled circles), chloride (squares), nitrate (triangles) as a function of irradiation time; (b) concentration profiles in mg C l^{-1} of CDNBA (filled circles) and DOC (open circles); ($[CDNBA]_0 = 5.0 \times 10^{-4}$ mol l^{-1}, i.e. 42 mg C l^{-1}, 350 ml annular photoreactor, see Section 2.2).

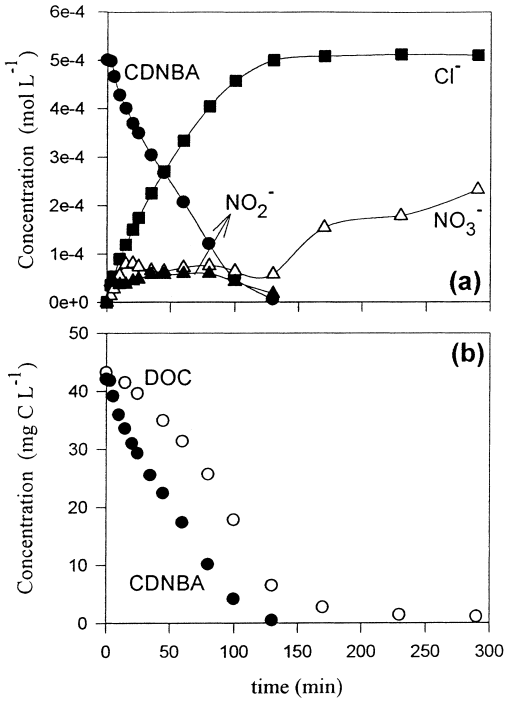

Fig. 7. Degradation of CDNBA by VUV photolysis of water at 185 nm: (a) concentration profiles in mol l^{-1} of CDNBA (filled circles), chloride (squares), nitrate (open triangles) and nitrite (filled triangles) as a function of irradiation time; (b) concentration profiles in mg C l^{-1} of CDNBA (full circles) and DOC (open circles); ($[CDNBA]_0 = 5.0 \times 10^{-4}$ mol l^{-1}, i.e. 42 mg C l^{-1}, 350 ml annular photoreactor, see Section 2.2).

in the UV/H_2O_2 process. Such a result was to be expected as the primary reaction responsible for CDNBA consumption is the same in the two processes (reaction with hydroxyl radicals). Only traces of NO_2^- could be detected under irradiation at 172 nm. In fact, irradiation of aerated aqueous solutions of NO_2^- at this wavelength leads to its efficient oxidation to NO_3^- [33]. Nitrate was formed in low amounts in the early stage of the reaction. Its concentration reached a maximum, decreased to trace amounts as CDNBA disappeared and could not be observed as long as DOC was present in solution (Fig. 6). This result is in agreement with previous reports showing that, when aerated aqueous solutions containing NO_3^- and organic matter are irradiated at 172 nm, NO_3^- is mainly reduced to NH_4^+ [33,36,37]. This reduction is initiated by the efficient reaction of NO_3^- with H atoms and solvated electrons, and involves a complex series of redox reactions and equilibria between nitrogen-containing ions and radicals, C-centered radicals and/or the organic substrate and its oxidation products. In the absence of dissolved organic matter, NH_4^+ is partially re-oxidized to NO_3^- [36,37].

In the case of the VUV photolysis at 185 nm, nitrite could be detected in low amounts. Its concentration reached a maximum and then decreased to zero when CDNBA was totally depleted. As NO_2^- disappeared, the NO_3^- concentration increased slowly, although the sum of NO_2^- and NO_3^- concentrations never exceeded 20% of the stoichiometric amount with respect to the initial organic nitrogen content in CDNBA. The differences observed in the evolution of NO_2^- and NO_3^- under photolysis at 172 and 185 nm, respectively, may be related to the lower quantum yield of H_2O homolysis and the larger irradiated volume in the latter case (Section 3.3.1). Under these conditions, the interplay of local concentrations of intermediate species, reaction rate constants, and diffusion rates leads to a less efficient oxidation of NO_2^- to NO_3^- during CDNBA degradation, as well as a less efficient reduction of NO_3^- to NH_4^+ when all CDNBA has been consumed (Fig. 7(a)).

4. Conclusion

Degradation of CDNBA in aqueous solution by photolysis is a very slow process. As already observed for a variety of organic contaminants, considerably faster degradation rates and complete mineralization could be achieved when CDNBA was oxidized by hydroxyl radicals produced either by UV-C photolysis of H_2O_2 or by VUV photolysis of water. Low or medium pressure mercury arcs were employed in the UV/H_2O_2 process, whereas VUV photolysis of water was carried out at 185 nm using a low pressure mercury arc with Suprasil envelope or at 172 nm employing a Xe-excimer lamp.

For the UV/H_2O_2 process, the optimal concentration of H_2O_2 leading to the fastest degradation rate could be evaluated as a function of the initial CDNBA concentration using a simplified equation based on the main reactions involved in the first stages of the degradation process. This optimal concentration represents the best compromise between two contradictory requirements, increase the fraction of incident radiation absorbed by H_2O_2 and therefore the production of hydroxyl radicals, and minimize the competitive trapping of hydroxyl radicals by H_2O_2 itself.

Under comparable experimental conditions (same reactor, same initial concentration of CDNBA, lamps of similar size), CDNBA was degraded significantly faster by the VUV process. Although energy consumption for the production of UV-C is comparatively smaller than that for the production of VUV radiation, the latter process presents several advantages, no additive is needed, thus avoiding competition between additive and substrate/products for the trapping of hydroxyl radicals, the whole incident radiation is absorbed by water and there are no inner filter effects due to the absorption of radiation by the substrate or its oxidation products.

Product analysis showed that, independently of the method used for the production of hydroxyl radicals, (i) no aromatic intermediates were formed in detectable amounts, indicating that ring opening should occur at an early reaction stage, (ii) chloride ions were produced at the same rate as CDNBA was depleted. This latter result confirms that the primary reaction responsible for CDNBA degradation

is the same in the VUV and UV/H_2O_2 processes. During the latter process, the amount of NO_3^- formed was close to the stoichiometric molar ratio that would be expected if all the CDNBA nitrogen content was mineralized to nitrate (two nitrate ions formed per molecule of CDNBA mineralized). The evolution of nitrogenated ions (nitrite and nitrate) during the VUV process was more complex, as a result of the production of primary reducing intermediates by VUV photolysis of water.

Acknowledgements

The collaboration between the two research groups was made possible by the DAAD-ANTORCHAS program and by the contract between the BMBF (DLR) and SECyT (project nr. ARG 027/98 ENT). The work in Argentina was partially supported by the Consejo Nacional de Investigaciones Científicas y Técnicas de la República Argentina (CONICET-PIP 4354), Agencia Nacional de Promoción de Ciencia y Tecnología (PICT 06-03531), the Comisión de Investigaciones de la Provincia de Buenos Aires (CICPBA) and the Universidad Nacional de La Plata (UNPL). F.G.E thanks the UNPL for a graduate-scholarship. The authors thank Tania Stingel and Frank Zegenhagen (Karlsruhe) for their contribution to the analytical work.

References

[1] O. Legrini, E. Oliveros, A.M. Braun, Chem. Rev. 93 (1993) 671.
[2] M. Doré, Chimie des Oxydants, Traitment des eaux, TEC & DOC, Paris, 1989.
[3] N. Clarke, G. Knowles, Effluent Water Treatment J. 9 (1982) 335.
[4] T. Oppenländer, G. Baum, W. Egle, EPA Newslett. 52 (1994) 53.
[5] M. Stefan, A. Hoy, J. Bolton, Env. Sci. Technol. 30 (1996) 2382.
[6] N. Takahasi, T. Nakai, Y. Satohi, K. Katho, O_3 Sci. Technol. 17 (1995) 511.
[7] C. Minero, E. Pelizzetti, P. Pichat, M. Saga, M. Vicenti, Env. Sci. Technol. 29 (1995) 2226.
[8] L. Jakob, T.M. Hashem, S. Bürki, N.M. Guindy, A.M. Braun, J. Photochem. Photobiol. A: Chem. 75 (1993) 97.
[9] M.C. Gonzalez, A.M. Braun, A. Bianco-Prevot, E. Pelizzetti, Chemosphere 28 (1994) 2121.
[10] M.C. Gonzalez, T.M. Hashem, L. Jakob, A.M. Braun, Fresenius J. Anal. Chem. 351 (1995) 92.
[11] P. Ho, Environ. Sci. Technol. 20 (1986) 260.
[12] S. Guittonneau, J. de Laat, M. Dore, J.P. Duguet, C. Bonnel, Environ. Tech. Lett. 9 (1988) 1115.
[13] Beilstein Organische Chemie, Syst no. 938, p. A416.
[14] B. Eliason, U. Kogelschatz, H.J. Stein, EPA Newslett. 32 (1988) 29.
[15] B. Gellert, U. Kogelschatz, Appl. Phys. B 52 (1991) 14.
[16] L. Jakob, Ph.D. thesis, Traitement des eaux par photocatalyse et photolyse V-UV: dégradation oxydative de polluants organiques, Ecole Polytechnique Fédérale de Lausanne, Switzerland, Thèse no. 1037, 1992.
[17] T.M. Hashem, Ph.D. thesis, The use of VUV and UV-C light sources for advanced oxidation processes, Universität Karlsruhe (TH), Germany, 1998.
[18] G. Heit, Ph.D. thesis, Entwicklung and Anwendung neuer Verfahren zur photochemischen Prozessanalyse, Universität Karlsruhe (TH), Germany, 1997.
[19] G. Heit, A. Neuner, P.-Y. Saugy, A.M. Braun, J. Phys. Chem. A 102 (1998) 5551, and references cited therein.
[20] A.M. Braun, M.-T. Maurette, E. Oliveros, Photochemical Technology, Wiley, Chichester, 1991, Chapter 2, pp. 75–77, and references cited therein.
[21] P. Griess, Chem. Ber. 12 (1889) 427.
[22] L. Ilosva von Ilosva, Bull. Soc. Chim. 3 (1889) 347.
[23] Y. Hasegawa, Chem. Lett. (1983) 129.
[24] D. Barton, W. D. Ollis, Nitrogen compounds, carboxylic acids, phosphorous compounds, in: O.D. Sutherland (Ed.), Comprehensive Organic Chemistry, Vol. 2, Pergamon Press, Oxford, 1981.
[25] J.R. Bolton, S.R. Cater, in: G. R. Helz, R. G. Zepp, D. G. Crosby, (Eds.), Aquatic and Surface Photochemistry, Lewis Publishers, Boca Raton, FL, 1994, pp. 467–490, and references cited therein.
[26] G.V. Buxton, C.L. Greenstock, W.P. Helman, A.B. Ross, J. Phys. Chem. Ref. Data 17 (2) (1988) 513.
[27] H. Christensen, K. Sehested, H. Corfitzen, J. Phys. Chem. 86 (1982) 1588.
[28] L. Ashton, G.V. Buxton, C.R. Stuart, J. Chem. Soc., Faraday Trans. 91 (1995) 1631.
[29] S. Guittonneau, J. de Laat, M. Doré, J.P. Duguet, H. Suty, Environ. Technol. 11 (1990) 57.
[30] P. Neta, L.M. Dorfman, Adv. Chem. Ser. 81 (1968) 222.
[31] D.F. Ollis, in: Proceedings of the Fifth International Conference on Advanced Oxidation Technologies for Water and Air Remediation, (#AOT-5), 1999, Albuquerque, USA.
[32] J.C. D'Oliveira, C. Minero, E. Pelizzetti, P. Pichat, J. Photochem. Photobiol. A: Chem. 72 (1993) 261.
[33] M. Gonzalez, A.M. Braun, Res. Chem. Intermed. 21 (1995) 837.
[34] J.L. Weeks, A.C. Meaburn, S. Gordon, Rad. Res. 19 (1963) 559.
[35] G. Heit, A.M. Braun, Water Sci. Technol. 35 (1997) 25.
[36] M. Gonzalez, A.M. Braun, J. Photochem. Photobiol. A: Chem. 93 (1996) 7.
[37] M. Gonzalez, A.M. Braun, J. Photochem. Photobiol. A: Chem. 95 (1996) 67.